Hindawi
Journal of Chemistry
Volume 2021, Article ID 7873488, 14 pages
https://doi.org/10.1155/2021/7873488

Research Article

Studies on the Removal of Cadmium Toxic Metal Ions by Natural Clays from Aqueous Solution by Adsorption Process

Rajaa Bassam,[1] **Achraf El hallaoui**,[2] **Marouane El Alouani**,[3] **Maissara Jabrane**,[1] **El Hassan El Khattabi**,[1] **Malika Tridane**,[1,4] **and Said Belaaouad**[1]

[1]*Laboratory of Physical Chemistry of Materials LCPM, Faculty of Sciences Ben M'Sik, Hassan II University of Casablanca, B.P.7955, Bd CdtDriss El Harti, Casablanca, Morocco*
[2]*Laboratory of Organic, Organometallic and Theoretical Chemistry, University Ibn Tofail, Faculty of Science, B.P. 133, Kenitra 14000, Morocco*
[3]*Laboratory of Physico-Chemistry of Inorganic and Organic Materials (LPCIOM), Materials Science Centre (MSC), Mohammed V University, Ecole Normale Supérieure (ENS), Rabat, Morocco*
[4]*Regional Center for Education and Training Occupations, Casablanca Anfa, Bd Bir Anzarane, Casablanca, Morocco*

Correspondence should be addressed to El Hassan El Khattabi; eelkhattabi36@gmail.com

Received 4 May 2021; Revised 7 July 2021; Accepted 15 September 2021; Published 12 October 2021

Academic Editor: Ajaya Kumar Singh

The aim of this study is the valorization of the Moroccan clays (QC-MC and QC-MT) from the Middle Atlas region as adsorbents for the treatment of water contaminated by cadmium Cd (II) ions. The physicochemical properties of natural clays are characterized by ICP-MS, XRD, FTIR, and SEM techniques. The adsorption process is investigated as a function of adsorbent mass, solution pH, contact time, temperature, and initial Cd (II) ion concentration. The kinetic investigation shows that the adsorption equilibrium of Cd (II) ions by both natural clays is reached after 30 min for QC-MT and 45 min for QC-MC and fits well to a pseudo-second-order kinetic model. The isotherm study is best fitted by a Freundlich model, with the maximum adsorption capacity determined by the linear form of the Freundlich isotherm being 4.23 mg/g for QC-MC and 5.85 mg/g for QC-MT at 25°C. The cadmium adsorption process was thermodynamically spontaneous and exothermic. The regeneration process showed that these natural clays had excellent recycling capacity. Characterization of the Moroccan natural clays before and after the adsorption process through FTIR, SEM, XRD, and EDX techniques confirmed the Cd (II) ion adsorption on the surfaces of both natural clay adsorbents. Overall, the high adsorption capacity of both natural clays for Cd (II) ions removal compared to other adsorbents motioned in the literature indicated that these two natural adsorbents are excellent candidates for heavy metal removal from aqueous environments.

1. Introduction

Cadmium is selected as a highly toxic inorganic pollutant to the environment or other living organisms. The environmental problem of cadmium is a consequence created by a human through their activities such as alloy in the automotive industry; as a pigment; as a stabilizer for plastics, in battery manufacturing, and nuclear reactors [1–3]. Several studies have shown that long-term use of water contaminated with this element causes adverse effects on human health [4, 5]. Considering the toxicity and adverse effects of cadmium on human health, the World Health Organization (WHO) fixed the maximum concentration of cadmium in drinking water at 0.03 mg/L [6].

The elimination of these types of pollutants is always a major challenge. Numerous studies have developed several treatment processes to reduce the amount of cadmium in aquatic environments [7–11]. The adsorption process is a better advantage rather the other methods due to their simplicity, low cost, and efficiency in removal of contaminants of a different nature in particular heavy metals [12, 13]. In addition, research and development of new natural

adsorbents which are abundant, economically profitable, and efficient for the treatment of ecosystems is a great challenge. In this context, the application of natural clay minerals is of great scientific interest. The adsorption of different pollutant by clays minerals has three types: the first is physical and nonionic adsorption, the second is ion exchange with electrostatic interaction and exchange reaction, and the third is zeolite action [14–17].

The objective of this work was to optimize the adsorption performance of cadmium by natural clays minerals, without any purification step, through its casting as adsorbent to replace expensive adsorbents used in the treatment of cadmium-polluted water. In particular, this study was focused on the elimination of cadmium in aqueous solution by retention onto local natural clays QC-MC and QC-MT collected from the Middle Atlas in the region of Khenifra, Morocco, and their ability to regenerate and be used again. QC-MC and QC-MT were selected based on their different physical and chemical properties such as chemical composition, nature of the oxygen and hydrogen surface atoms, defect sites, layer charge, and the type of exchangeable cations. Moreover, they were also selected according to their originality. QC-MC and QC-MT have never been the subject of a structural and mineralogical study allowing the knowledge of their nature and their performance over the adsorption of cadmium ions. Therefore, this work ensures the determination of the physicochemical properties of QC-MC and QC-MT. Hence, we studied the performance of cadmium adsorption selected as an inorganic pollutant. The removal of cadmium using QC-MC and QC-MT was carried out by varying several parameters such as adsorbent mass, pH of the solution, initial concentration of cadmium, contact time, and temperature. The kinetic, isotherm, and thermodynamic studies were investigated. The regeneration study was also examined by using different acids.

2. Materials and Methods

2.1. Reagents. All chemical reactants were of high analytical quality and were applied without further distillation, which was obtained from the LaboChimie Society. All solutions were prepared with high purity deionized water. In addition, all glassware was washed by soaking in 10% HCl and rinsed three times with deionized water. The Cd (II) stock solution was prepared from cadmium chloride ($CdCl_2.H_2O$).

2.2. Preparation and Characterization of Adsorbents. QC-MC and QC-MT were collected from the Middle Atlas Mountains of Morocco and were used as adsorbents to remove cadmium cations. QC-MC and QC-MT were ground and sieved, and the fraction contains 500 µm and was used in this study without any further pretreatment. The X-ray diffraction (XRD) detected the mineralogical composition using BRUKER-Binary V4, the Fourier transform infrared (FTIR) was used to determine the grouping structural of adsorbents which was executed by SHIMADZU8400S, the inductively coupled plasma mass spectrometry (ICP-MS) allows the determination of a wide range of inorganic elements and elementary impurities, in one go, with extreme reliability and precision, the scanning electron microscopy (SEM) was used to provide the detailed high-resolution image with Zeiss model, the cation exchange capacity (CEC) parameter has been made at the free pH of the suspensions by the cobalt hexamine method, the porosity was affected by the mercury intrusion porosimeter method recorded on Quantachrome Mercury POREMASTER, and the point of zero charges (PZC) was determined using a drift method.

2.3. Batch Adsorption Studies. A batch test was conducted to investigate Cd (II) adsorption at several effects pH of the solution, concentration, mass, contact time, and temperature. The pH was adjusted by adding HCl (1M) or NaOH (1M). The solution of adsorption Cd (II) was shaken at 450 rpm. After the adsorption reaction, the suspension was centrifuged for 10 min at 3 500 rpm and then filtered. The Cd (II) concentration in an aqueous solution was revealed by ICP-MS using the PerkinElmer model. The quantity of cadmium (II) adsorbed is intended by the following equation:

$$Q_e = \frac{v(C_0 - C_e)}{m}, \tag{1}$$

where Q_e is the capacity of Cd (II) adsorbed at equilibrium (mg/g), C_o is the initial concentration of cadmium (mg/L), C_e is the concentration of cadmium in equilibrium (mg/L), m is adsorbents dose (g), and V is solution volume (L).

2.4. Isotherm Modeling. Adsorption isotherms are experimental curves that represent variation in adsorbed metal ions by adsorbent as a function of concentration. They are generally expressed in the form of mathematical equations. The equilibrium isotherm analysis was affected by applying two models: Langmuir and Freundlich [18].

The Langmuir isotherm theory supposes that adsorption is a monolayer and occurs at homogeneous sites specific to the adsorbent. The linear equation from the Langmuir equation is expressed as

$$\frac{C_e}{Q_e} = \frac{1}{K_L.Q_{\max}} + \frac{C_e}{Q_{\max}}, \tag{2}$$

where K_L is the equilibrium constant comparative to the Langmuir model and $Q_{\max}$ is the maximum amount adsorbed of Cd (II) (mg/g). The $Q_{\max}$ and K_L are determined from the drift.

The Freundlich isotherm presumes that adsorption is multilayer and the adsorbent surface is heterogeneous. It can be confirmed by the following equation:

$$LnQ_e = LnK_F + \frac{LnCe}{n}, \tag{3}$$

where K_F (L/g) and n are the Freundlich constants representing the adsorption and intensity, respectively.

2.5. Kinetic Modeling. The kinetic study permits us to examine the impact of contact time on its retention. Usually, kinetic results allow us to determine the rate and mechanism

of adsorption. In this study, two models were applied to describe the mechanism of kinetic adsorption of Cd (II) on adsorbents: the pseudo-first-order and the pseudo-second-order [19].

The pseudo-first-order kinetic model is presented by Lagergren in the equation:

$$\ln(Q_e - Q_t) = \ln(Q_e) - K_1.t, \quad (4)$$

where Q_t (mg/g) and Q_e (mg/g) are the capacities of cadmium ion adsorbed at time t and equilibrium, respectively. K_1 (min^{-1}) is the pseudo-first-order constant.

The pseudo-second-order model is defined by the supposition that the correlation of occupation of adsorption sites is corresponding to the square of the number of unoccupied sites and is indicated in its linear form as follows:

$$\frac{t}{Q_t} = \left(\frac{1}{Q_e}\right).t + \frac{1}{K_2 Q_e^2}, \quad (5)$$

where K_2 (g/mg.min) is the pseudo-second-order constant.

2.6. Intraparticle Diffusion. Weber and Morris presented this model in equation (6); K_w and constant C values can be resolute from the graph and of order at the origin of the Q_t curve as a function of $t^{t1/2}$:

$$Q_t = K_w t^{1/2} + C. \quad (6)$$

2.7. Thermodynamic Study. The determination of thermodynamic parameters is very important to understand the effect of temperature on adsorption. It also ensures in principle to predict the strength of the bonds between the adsorbent and the adsorbate. The thermodynamic parameters including the free energy (ΔG°), the standard enthalpy (ΔH°), and the standard entropy (ΔS°) can be calculated by the following equations:

$$\Delta G^\circ = -RT\left(\ln \frac{Q_e}{C_e}\right),$$

$$K_d = \frac{Q_e}{C_e}, \quad (7)$$

$$\ln K_d = \frac{\Delta S^\circ}{R} - \frac{\Delta H^\circ}{RT},$$

where R is the perfect gas constant (8.314 J/mol. K), T is the temperature in Kelvin (K), and K_d is the distribution coefficient of the solute in the adsorbent and the solution.

2.8. Regeneration of QC-MC and QC-MT. Adsorbent regeneration is an important process for low-cost treatment of adsorbents to recycling again. In this study, the contaminated QC-MC and QC-MT were regenerated by three different acids including nitric acid (3M), hydrochloric acid (3M), and sulfuric acid (3M). The mixture was shaken for one hour at 450 rpm. The desorption process was analyzed for four cycles.

3. Results and Discussion

3.1. Characterization of Adsorbents

3.1.1. X-Ray Diffraction. The XRD patterns of QC-MC and QC-MT are given in Figure 1. It was noted that the characteristic diffraction peaks of QC-MC detect the presence of Quartz in the lattice plans of (100), (101), (112), (110), (211), and (301); calcite in three peaks (104) and (113); and the presence of mica in the peaks (020) and (114). The QC-MT sample shows the presence of Quartz in the plans (100), (101), (111), (200), (202), (103), (112), (211), (301); the peaks of (104) and (113) detected the presence of calcite; the montmorillonite was also detected in QC-MT in the plans (020), (060), and (130). The mineralogical composition of QC-MC and QC-MT has a similar structure.

3.1.2. Inductively Coupled Plasma Mass Spectrometry. To determine the content of each component of the samples studied, an ICP-MS analysis was carried out. ICP-MS is an elementary technique based on the mass spectrometry analysis of ions generated by the inductively coupled plasma. ICP-MS results for QC-MC and QC-MT are shown in Table 1. The QC-MC contains rich elements such as iron, silicon, magnesium, potassium, aluminum, calcium, and sodium, but also low-grade elements, for example, strontium, selenium, thallium, vanadium, and manganese. On the other hand, silicon, magnesium, potassium, aluminum, calcium, and sodium are also enriched in QC-MT; other elements contained in QC-MT are low concentrations, such as iron, strontium, selenium, thallium, vanadium, and manganese. These results confirm those found by XRD and FTIR.

3.1.3. Physicochemical Properties of Adsorbents. The physicochemical properties of the samples determined in this study are cation exchange capacity (CEC), humidity, and porosity. The principle of measurement is to move all adsorbed cations to the exchange sites and to saturate the sites by a single cation; the cationic exchange capacity is defined as the number of monovalent cations capable of substituting the 100 g cations of the solid. Large CEC values of 148.8 me/100 g and 145.6 me/100 g were detected for the QC-MC and QC-MT, respectively, which signified the swelling character. Moisture consists of detecting the mass of water removed by drying in a moisture analyzer, and the results of the moisture are 2.89% and 1.75% for QC-MC and QC-MT, respectively. Porosity is a macroscopic quantity that allows quantifying of the unoccupied volume by the solid, the QC-MC, and QC-MT, defined by a medium porosity of 65% and 70%, respectively.

3.1.4. Point of Charge Zero. The PZC is an important parameter that represents an estimate of its acidobasicity; generally, it is used to describe variable-charge surfaces of solids. The activities of potential ions (H^+ and OH^-) and the electrolyte concentrations are influenced by the surface charge of adsorbents. In this study, the PZC was determined at the point of intersection of the titration drift at different

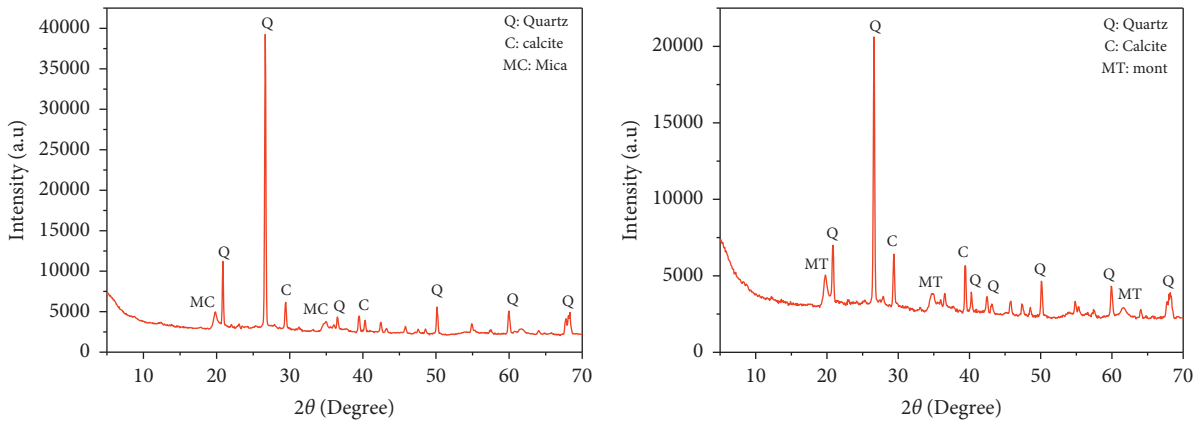

(a) (b)

Figure 1: XRD patterns for (a) QC-MC and (b) QC-MT.

Table 1: Elemental composition of QC-MC and QC-MT determined by ICP-MS.

Clay (%)	SiO_2	Na_2O	Al_2O_3	MgO	Fe_2O_3	K_2O	CaO	Other
QC-MC	45	6	2	4	1	4	36	2
QC-MT	53	11	1	3	0	7	24	1

ionic forces (Figure 2). As a result, the PZC of QC-MC and QC-MT are 8.7 and 8.5, respectively. The convergence PZC values of the adsorbents studied show that the structural composition of QC-MC and QC-MT is approximately comparable and the functional groups are of similar surfaces, which explain the resemblance of the PZC curves. The pH of QC-MC and QC-MT in the reaction medium is basic, which means that the surface of QC-MC and QC-MT has basic functions such as oxygen groups. The FTIR spectra of QC-MC and QC-MT represent different functional groups of these materials. QC-MC and QC-MT PZC curves are similar to other studies [20–22]. Therefore, the difference between acid and basic pH is very large for QC-MC and QC-MT. That signified a high electrostatic attraction present between the OH^- ions and the cationic adsorbates. Therefore, it can be concluded that QC-MC and QC-MT are capable of fixing Cd (II) on their surface at a pH greater than pH_{pzc}.

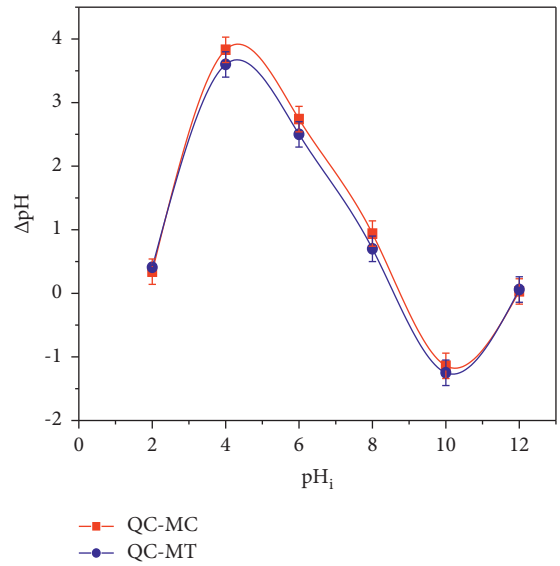

Figure 2: PZC drift for (a) QC-MC and (b) QC-MT.

3.2. Adsorption Procedure

3.2.1. Effect of Time. The effect of contact time on the elimination rate of Cd (II) ions has been studied on a range of 1 min to 180 min and the variation on adsorption capacity as shown in Figure 3 with an initial concentration of Cd (II) ions is 10 mg/L, and an adsorbents dose of 1.5 g at room temperature (25°C) and pH of the solution is 5 for QC-MC and QC-MT. The results obtained show that the elimination rate increases rapidly to reach equilibrium in 45 min for QC-MC; the removal rate of Cd (II) ions on QC-MT was increasing during the 30 min and then remains almost constant, equivalent to the adsorption capacity of 4.17 mg/g for QC-MC and 5.49 mg/g QC-MT. Therefore, the slow increase of the Cd (II) ions elimination rate up to the equilibrium time indicates that there is an internal mass transfer of the adsorbent; this mostly relates to a phenomenon of diffusion in the internal porosity of the adsorbent.

3.2.2. Effect of Mass. The influence of adsorbent mass was explored between 0.1 and 4 g. The concentration initial of Cd (II) ions is 10 mg/L, and the contact time is 45 min for QC-MC and 30 min for QC-MT at pH of solution 5 for QC-MC and QC-MT. The curve in Figure 4 shows that a mass of 1.5 g of QC-MC and QC-MT is capable of setting maximum Cd (II) ions of the order of 3.98 mg/g for QC-MC and 5.21 mg/g for QC-MT. To ensure an equivalent number of adsorption sites, the quantities of Cd (II) ions fixed must be following the doses of adsorbent in the solution. Beyond a certain mass, the retention rate remains constant slightly indicating the saturation of the adsorbent surface. Therefore, it is useful to work with doses of adsorbent 1.5 g and an ineffective overdose is avoided.

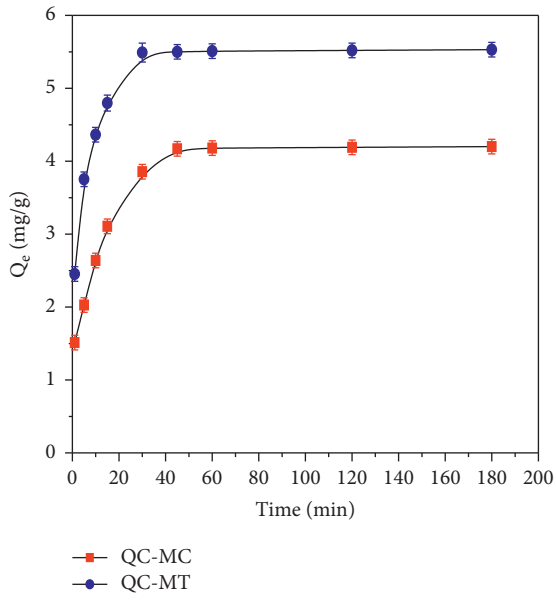

Figure 3: Effect of contact time of Cd (II) on QC-MC and QC-MT ($C_0 = 10$ mg/L, $T = 25$°C, $m = 1.5$ g, $V = 100$ mL, and pH = 5).

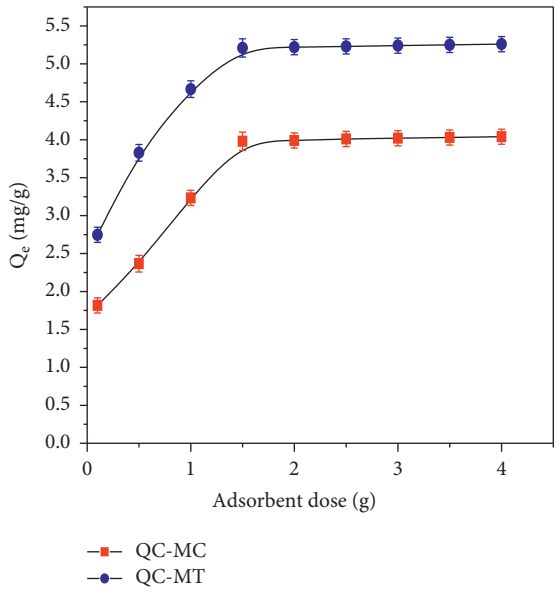

Figure 4: Effect of adsorbent mass of removal of Cd (II) ions ($V = 100$ mL, $T = 25$°C, $C_0 = 10$ mg/L, contact time = 45 min for QC-MC and 30 min for QC-MT, and pH = 5).

3.2.3. Effect of pH. The pH of the medium conditions the state of the surface charge as well as the adsorbent adsorbate. The initial concentration of cadmium was fixed at 10 mg/L and the adsorbents dose is 1.5 g in 45 min for QC-MC and 30 min for QC-MT of contact time at room temperature 25°C. Figure 5 shows a high removal of Cd (II) ions in pH = 5 for QC-MC and QC-MT, with the values of rate increases of 4.15 mg/g for QC-MC and 5.36 mg/g for QC-MT. However, at alkaline medium, the concentration of Cd^{2+} decreases due to the formation of Cd $(OH)_2$. As a result, it was obvious that the best adsorption of cadmium onto QC-MC and QC-MT is favorable at an acid medium.

3.2.4. Effect of Initial Concentration of Cd (II). For analysis of the effect of Cd (II) concentration on adsorption capacity, the contact time of Cd (II) ions is 45 min for QC-MC and 30 min for QC-MT, the pH of the solution is 5, and the adsorbent dose is 1.5 g. The process was performed with different initial Cd (II) concentrations between 5 and 120 mg/L. As shown in Figure 6, adsorption efficiency increases when the initial high Cd (II) concentration reaches a constant value of 4.15 mg/g for QC-MC at 5.75 mg/g for QC-MT. All Cd (II) ions present in the adsorption medium may interact with the binding sites on the adsorption surface, such as at higher concentrations; adsorption yield is stable due to saturation of adsorption sites.

3.2.5. Isotherm Adsorption. The tracing of the retention isotherms gives information on the maximum adsorption capacity and the adsorption mechanism. The study was carried out with different initial concentrations at 25°C temperature, the contact time 45 min for QC-MC and 30 min for QC-MT at adsorbents dose is 1.5 g, and the pH of the solution is 5 for QC-MC and QC-MT, respectively. The drifts show the change in the amount adsorbed at equilibrium as a function of the equilibrium concentration $Q_e = f(C_e)$ (Figure 7).

The corresponding isotherm adsorption parameters are summarized in Table 2, which was deduced from Langmuir and Freundlich curves (Figure 7). The numerical value of n indicates that adsorption of Cd (II) ions is favorable for both adsorbents, and the correlation coefficient values for Freundlich were higher than those of Langmuir for QC-MC and QC-MT. The Freundlich equation can best describe the removal of Cd (II) using QC-MC and QC-MT, which suggests that the surfaces of QC-MC and QC-MT are heterogeneous and the adsorption of Cd (II) ions is made of the multilayer. These results show that the maximum amount of retention of Cd (II) ions was 4.23 mg/g for QC-MC and 5.85 mg/g for QC-MT.

3.2.6. Kinetics of Adsorption. The kinetics of adsorption are essential for evaluating and discussing the mechanism of fixation of the solute on the adsorbent surface and for describing the adsorption rate; with an initial concentration of 10 mg/L at 25°C temperature, the adsorbent dose is 1.5 g, and the pH = 5. In this context, two models have been applied to describe the mechanism of kinetic adsorption of Cd^{2+} onto QC-MC and QC-MT, pseudo-first-order, and pseudo-second-order (Figure 8).

The kinetic constants for both adsorbents are given in Table 3. According to the comparison of correlation coefficient (R^2), the pseudo-second-order values are higher than pseudo-first-order for QC-MC and QC-MT. Therefore, the adsorption of Cd (II) onto QC-MC and QC-MT followed the pseudo-second-order model, which signified that the adsorption mechanism is of a chemical nature (chemisorption) involving valence through the sharing or exchange of electrons between QC-MC and QC-MT adsorbents and Cd (II) ions, and the interaction and the retention of Cd (II) ions would be strong.

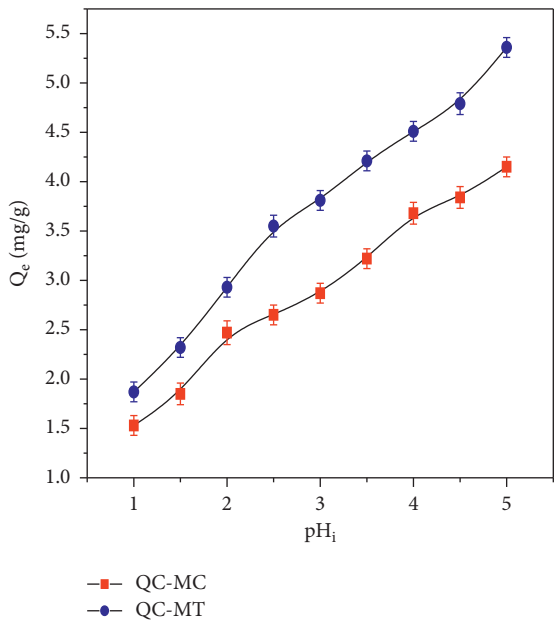

Figure 5: Effect of pH on Cd (II) removal by QC-MC and QC-MT ($C_0 = 10$ mg/L, $V = 100$ mL, $T = 25^{\circ}$C, $m = 1.5$ g, and contact time = 45 min for QC-MC and 30 min for QC-MT).

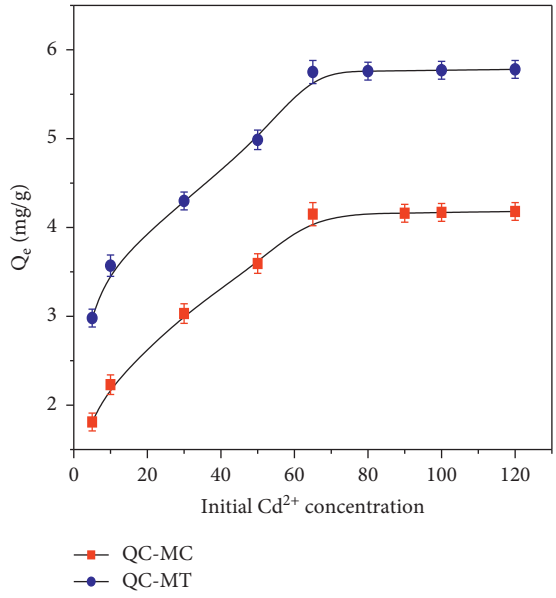

Figure 6: Effect of initial concentration of Cd (II) ions for QC-MC and QC-MT ($V = 100$ mL, $T = 25^{\circ}$C, $m = 1.5$ g, contact time = 45 min for QC-MC and 30 min for QC-MT, and pH = 5).

3.2.7. Intraparticle Diffusion. The intraparticle diffusion model was also used to describe the adsorption mechanism of several solid-liquid systems. This model assumes that the process of intraparticle diffusion is the limiting step that controls the rate of transfer of a solute from an aqueous phase to a solid phase. The intraparticle diffusion model plot is shown in Figure 9 for QC-MC and QC-MT. From the results, the multilinearity of Cd (II) ions adsorption on QC-MC and QC-MT adsorbents suggests that the entire adsorption process can be separated into three steps. The first step characterizes the transfer of Cd (II) ions from the aqueous solutions to the external surface of the QC-MC and QC-MT (film diffusion). The second step describes the transfer of Cd (II) ions from the external surface to the pores of the clay (intraparticle diffusion). The third step represents the fixation of Cd (II) ions to the surface of QC-MC and QC-MT (Adsorption). From Figure 9, the rate constant values of the intraparticle diffusion model of the second step (K_2) are higher than those of the first (K_1) and third (K_3) steps for QC-MC and QC-MT adsorbents. The kinetic data indicate that the Cd (II) ions adsorption on both natural clays is rapid during the second step, revealing that the adsorption rate was controlled by intraparticle diffusion.

3.2.8. Thermodynamic Study. Temperature is one of the important and effective parameters in the adsorption process. Figure 10 represents the variation in the maximum amount adsorbed from Cd (II) by QC-MC and QC-MT. According to the results, QC-MC and QC-MT exhibit similar behavior. It is observed that the adsorbed amount of QC-MC and QC-MT decreases slightly with temperature increase reflecting the exothermic nature of adsorption.

Thermodynamic parameters obtained are summarized in Table 4. According to the results, the values of the standard enthalpy ΔH° of QC-MC and QC-MT are negative which confirms that the process of adsorption of Cd (II) by QC-MC and QC-MT is exothermic. A negative ΔS° entropy value was found for QC-MC and QC-MT which means that Cd (II) molecules are more organized at the solid/liquid interface than in the liquid phase for these systems. The negative values of ΔG° obtained reveal that the adsorption process is favorable and that it is spontaneous and it was observed that ΔG° values increase slightly with temperature for QC-MC and QC-MT which reflects the negative effect of temperature on adsorption of Cd (II).

3.2.9. Regeneration of QC-MC and QC-MT. Adsorbent regeneration is considered an important economic aspect in reducing treatment costs. The regeneration of QC-MC and QC-MT polluted by Cd (II) was affected using the acid method, and the results are presented in Figure 11. After the regeneration cycles of QC-MC and QC-MT, the percentage desorption of Cd (II) by nitric acid was 18% for QC-MC and 15% for QC-MT, whereas hydrochloric acid was desorbed 21% for QC-MC and 25% for QC-MT, and sulfuric acid was reduced to 11% for QC-MC and 10% for QC-MT. However, the results of the regeneration of QC-MC and QC-MT show that hydrochloric acid is the most effective for the desorption of Cd (II) ions.

3.3. Characterization of Adsorbents after Adsorption

3.3.1. X-Ray Diffraction. According to Figure 12, after adsorption of Cd (II) by QC-MC and QC-MT, two broad peaks, which are centered at (002) with an interlayer distance $d_{(002)} = 2.56$ Å for QC-MC and at (103) with an interlayer distance $d_{(103)} = 1.50$ Å for QC-MT, are due to the presence of the Cd (II) ions. Following the spectra XRD,

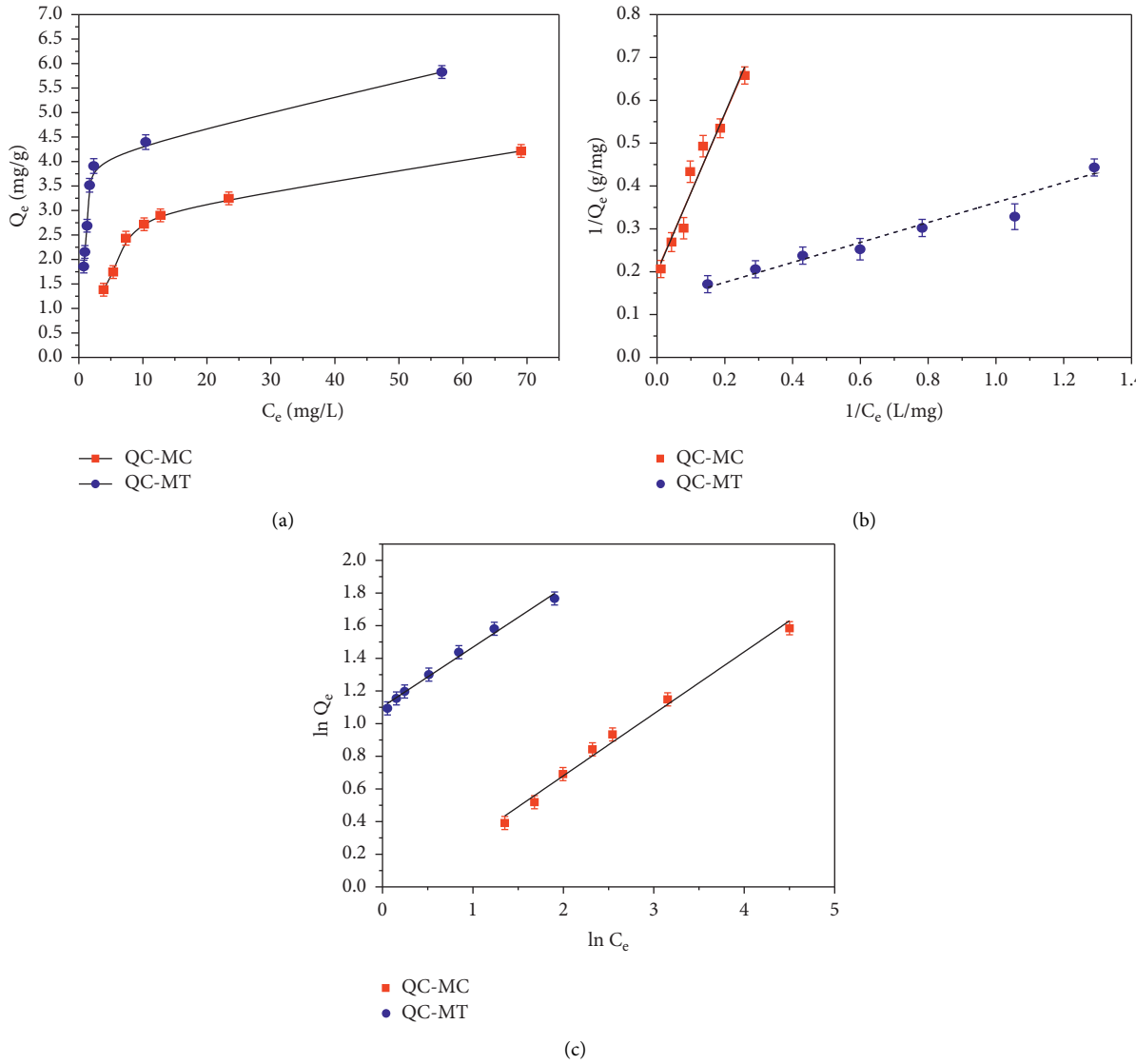

Figure 7: Adsorption isotherm for removal of Cd (II). (a) Isotherm curve and (b) Langmuir and (c) Freundlich models ($V = 100$ mL, $T = 25^{\circ}$C, $m = 1.5$ g, contact time = 30 min for QC-MC and 45 min for QC-MT, and pH = 5).

Table 2: Parameters of adsorption isotherm model.

Adsorbent	Langmuir constants			Freundlich constants		
	Q_{max} (mg/g)	K_L (L/g)	R^2	K_F (mg/g)	n	R^2
QC-MC	4.23	1.71	0.94	0.10	1.47	0.97
QC-MT	5.85	1.83	0.95	0.41	2.11	0.99

it was noticed that there is no change in the bands of mica for QC-MC and the montmorillonite for QC-MT; therefore, it can suggest that the Cd (II) ions were adsorbed on the surface of QC-MC and QC-MT.

3.3.2. Fourier Transform Infrared Spectroscopy. The FTIR spectra before and after adsorption of Cd (II) by QC-MC and QC-MT are presented in Figure 13. A large broad absorption around 3380–1639 cm^{-1} represents asymmetrical stretching and bending vibrations of the OH group, respectively.

The FTIR spectra of QC-MC confirm the existence of Quartz in the peaks 1038 cm^{-1}, 983 cm^{-1}, and 779 cm^{-1} which are due to Si-O symmetric stretching and bending [23–25]. Calcite was also detected in QC-MC at 1425 cm^{-1} and 1246 cm^{-1}, which are signified to doubly degenerate asymmetric stretching and C=O stretching, respectively [25, 26]; the frequency of 876 cm^{-1} is due to Al-O-H stretching mode vibration signified to the presence of mica [27, 28].

The infrared spectrum of QC-MT is characterized by several bands, the frequencies of Si-O symmetric stretching and bending at 1058 cm^{-1}, 986 cm^{-1}, and 778 cm^{-1} are due

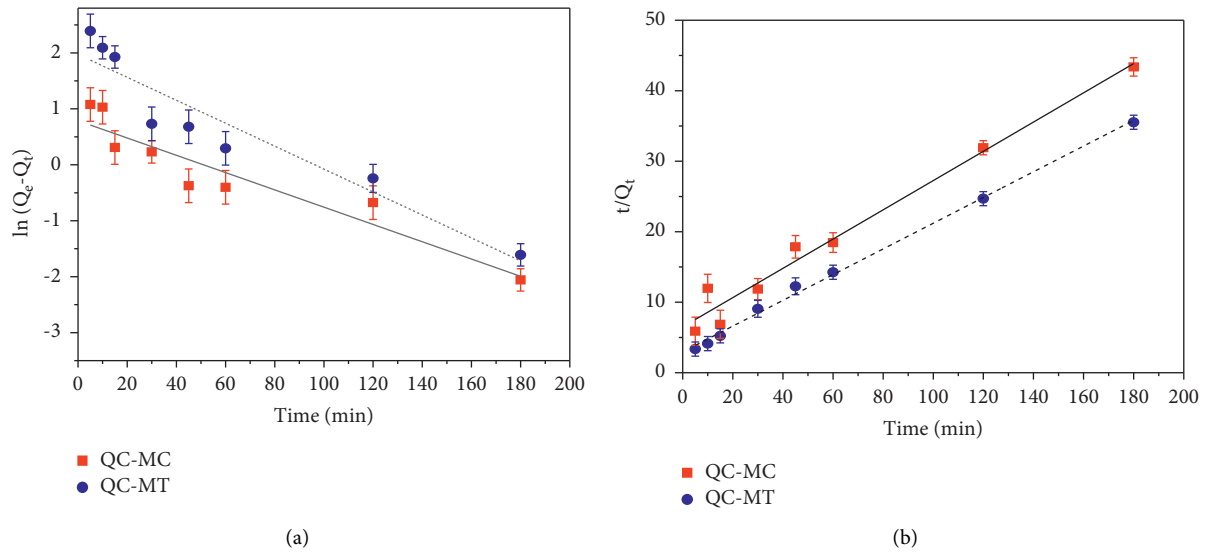

Figure 8: Kinetic models for adsorption of Cd (II) on QC-MC and QC-MT. (a) PFO and (b) PSO ($V = 100$ mL, $T = 25^{\circ}$C, $C_0 = 10$ mg/L, $m = 1.5$ g, and pH = 5).

Table 3: Kinetic parameters of QC-MC and QC-MT.

Adsorbent	T (°C)	Pseudo-first-order		Pseudo-second-order	
		K_1 (min^{-1})	R^2	K_2 (g/mg.min)	R^2
QC-MC	25	0.025	0.86	0.28	0.97
QC-MT		0.047	0.89	0.75	0.99

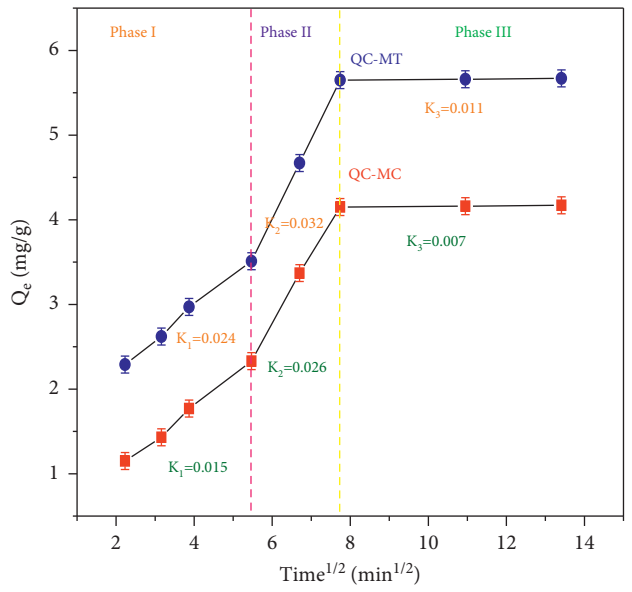

Figure 9: Intraparticle diffusion model of QC-MC and QC-MT ($V = 100$ mL, $T = 25^{\circ}$C, $C_0 = 10$ mg/L, $m = 1.5$ g, and pH = 5).

to the presence of Quartz (Ko, T.H. and Chu, H., 2005), montmorillonite was also present in QC-MT at 843 cm^{-1} which is due to Al-Mg-OH bending [26, 29], the FTIR spectroscopy detects the presence of calcite at 1451 cm^{-1} due to doubly degenerate asymmetric stretching, and 1247 cm^{-1} is due to C=O stretching in QC-MT [30, 31].

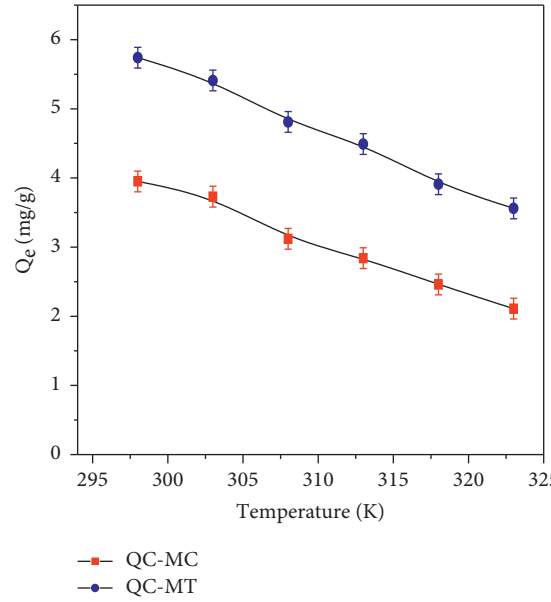

Figure 10: Effect of temperature on adsorption ($V = 100$ mL, $C_0 = 10$ mg/L, $m = 1.5$ g pH = 5, and contact time = 30 min for QC-MC and 45 min for QC-MT).

After adsorption of Cd (II) ions, the FTIR spectra remained largely unchanged, indicating that QC-MC and QC-MT have good stability and hence the potential for high reusability. The absorption peak was the same in QC-MC and QC-MT; it was observed at 549 cm^{-1}, which was caused by Cd (II) ions Cd-O stretching vibrations.

3.3.3. Scanning Electron Microscopy. The scanning electron microscopy was affected to analyze the texture and characterize mineralogical assemblies of the samples. Figure 14 presents the images of SEM with different enlargements of

Table 4: Thermodynamic parameters for the adsorption of Cd (II) ions.

	Temperature (K)	ΔS° (kJ/mol/K)	ΔH° (kJ/mol)	ΔG° (kJ/mol)
QC-MC	298	−0.1349	−41.247	−1.0468
	303			−0.3723
	308			0.3022
	313			0.9767
	318			1.6512
	323			2.3257
QC-MT	298	−0.1772	−56.759	−3.9534
	303			−3.0674
	308			−2.1814
	313			−1.2954
	318			−0.4094
	323			−0.4766

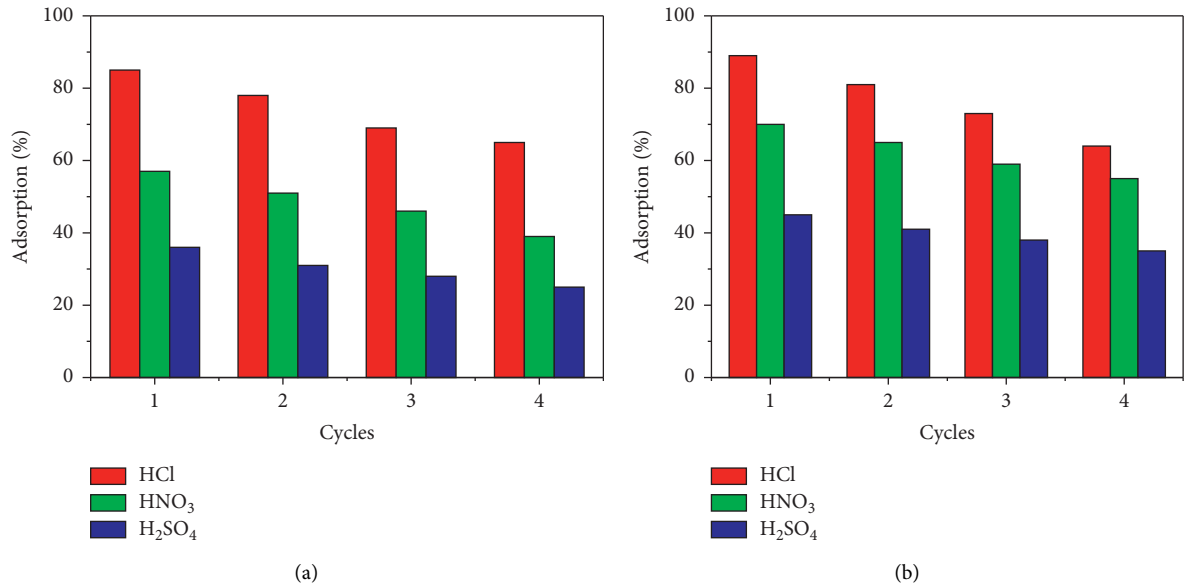

Figure 11: The regeneration of (a) QC-MC and (b) QC-MT ($V = 100$ mL, $m = 1.5$ g, $T = 25^{\circ}$C, and contact time = 30 min for QC-MC and 45 min for QC-MT).

QC-MC and QC-MT before and after adsorption of Cd (II), respectively. The adsorbent particles are in the form of clusters of fine aggregates and wafers in the shape of rods with irregular contours. The crystal structure layers were observed in the two adsorbents (Figure 14). From the SEM images and what was obtained in XRD, there is no doubt about the presence of calcite and Quartz in both samples, and the presence of Mica in QC-MC and the montmorillonite in QC-MT. Calcite is in the form of visible aggregates whereas Quartz is represented by small grains. Meanwhile the aggregates observed after adsorption of Cd (II) (Figure 14) were more probably to be indicative of Cd (II) ions adsorbed onto the surface of QC-MC and QC-MT.

3.3.4. Energy Dispersive X-Ray. The EDX analysis of QC-MC and QC-MT after adsorption of Cd (II) is presented graphically in Figure 15. The EDX patterns show the existence of iron, silicon, magnesium, potassium, aluminum, calcium, and sodium on the surface of QC-MC and the distribution of silicon, magnesium, potassium, aluminum, calcium, and sodium on the surface of QC-MT. These results are adapted to those obtained by the previous analyses. The sharp peaks at 0.2, 3.4, and 3.6 Kev for QC-MC and 0.1 and 3.5 Kev for QC-MT are attributed to Cd (II) adsorbed in the surface of these adsorbents. EDX analysis confirms the presence of Cd (II) on the surface of adsorbents, resulting from the adsorption of Cd (II) ions by QC-MC and QC-MT.

3.4. Comparative Study. Depending on these results, QC-MT can adsorb Cd (II) with an adsorption capacity of 5.85 mg/g in 30 min compared to QC-MC with an adsorption capacity of 4.23 mg/g in 45 min. The difference adsorption capacities of Cd (II) return to the difference in composition of each adsorbent.

The main types of adsorbents minerals on which Cd (II) will adsorb are such as silicates (silica, quartz, feldspar, etc.),

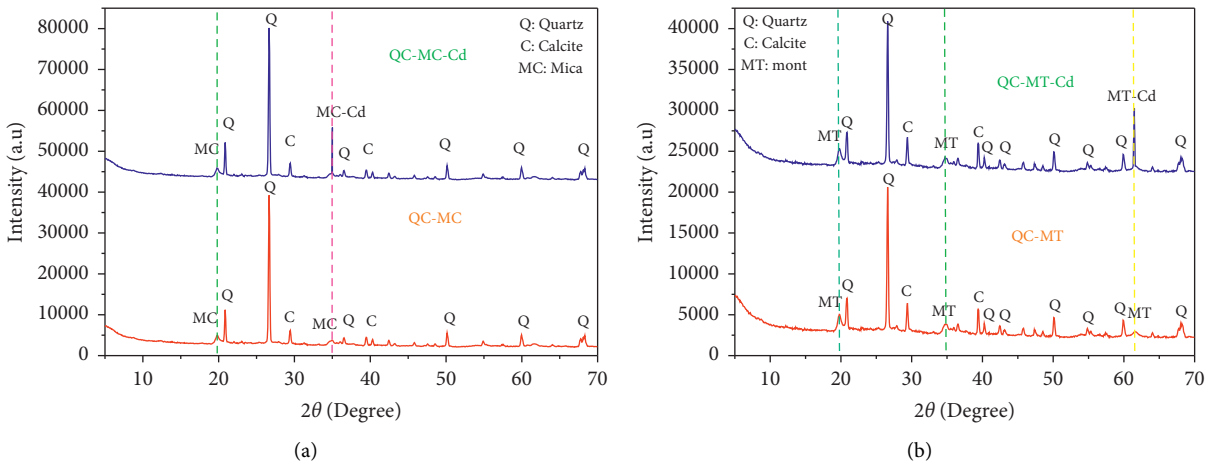

Figure 12: XRD pattern before and after adsorption of Cd (II) by (a) QC-MC and (b) QC-MT.

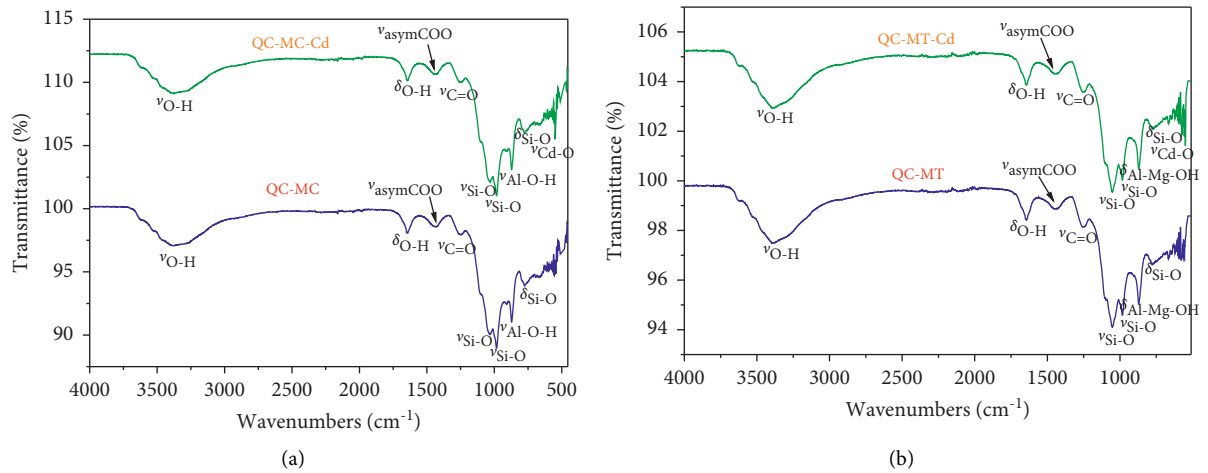

Figure 13: FTIR spectra before and after adsorption of Cd (II) by (a) QC-MC and (b) QC-MT.

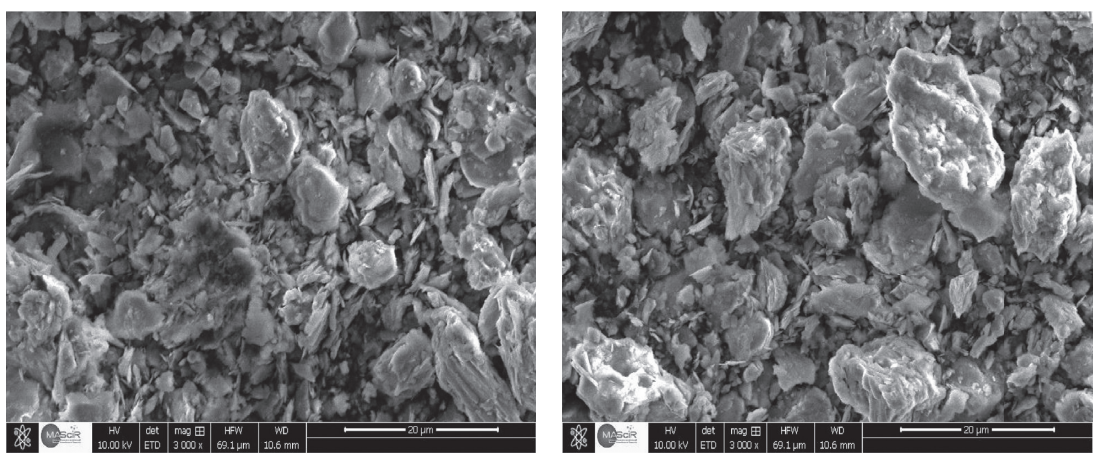

(a) (b)

Figure 14: Continued.

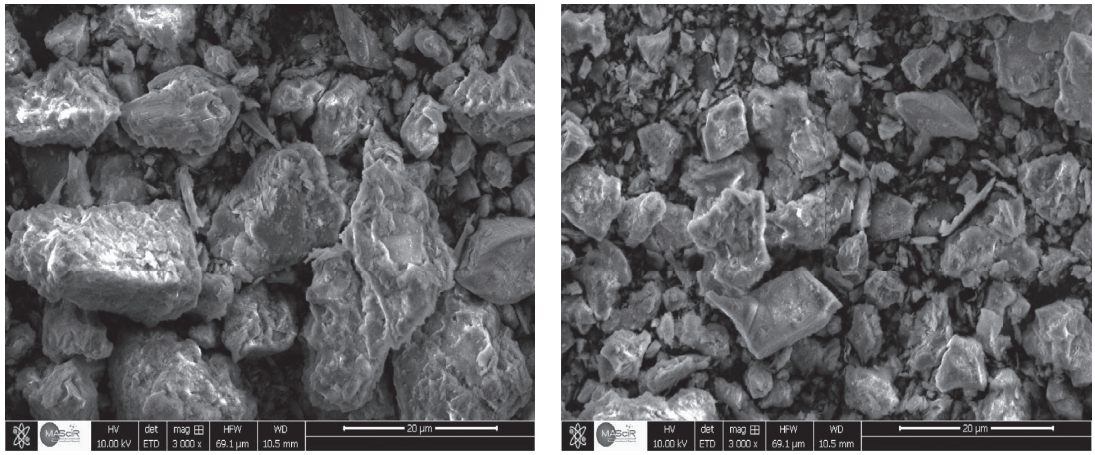

(c) (d)

Figure 14: SEM observations of (a, b) before and after adsorption onto QC-MC and (c, d) before and after adsorption onto QC-MT.

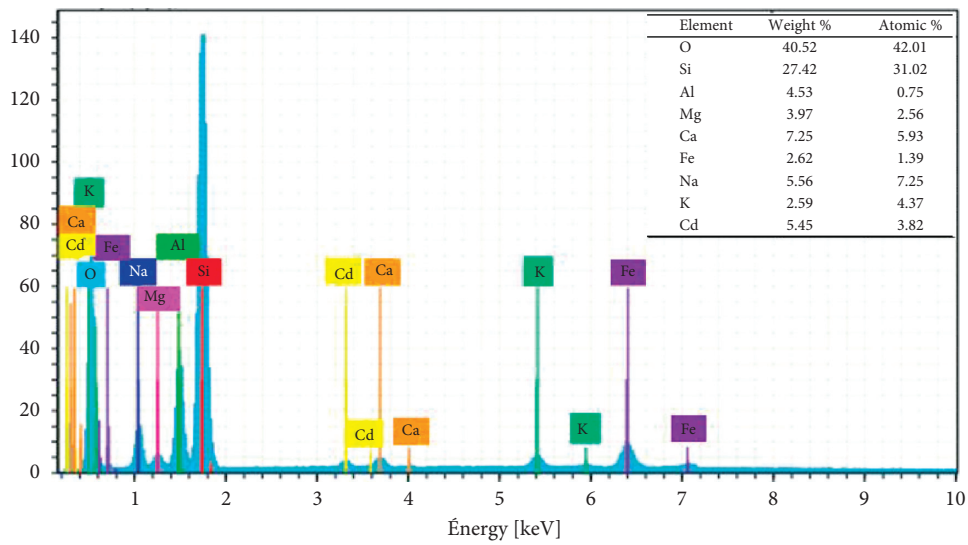

(a)

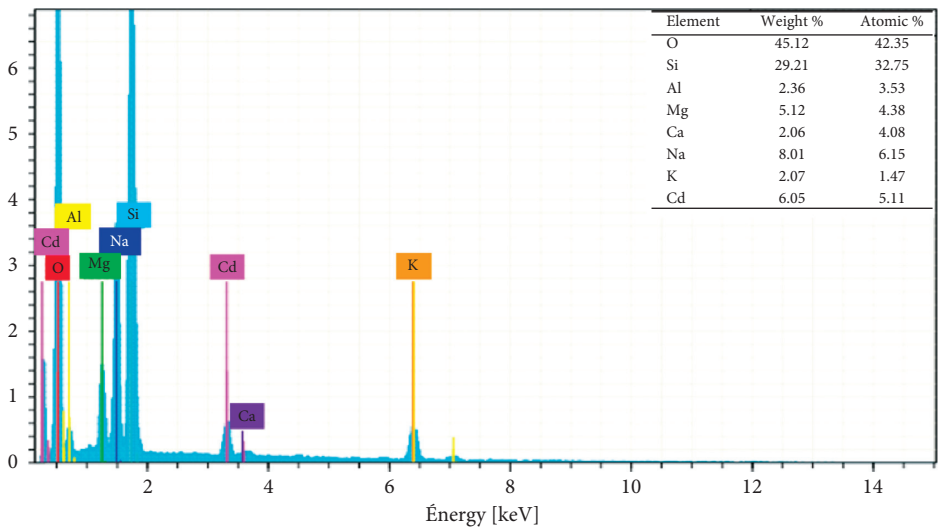

(b)

Figure 15: EDX analysis of (a) QC-MC and (b) QC-MT after adsorption of Cd (II).

Table 5: Comparison of adsorption capacities of Cd (II) on various adsorbents.

Adsorbent	Q_{max} (mg/g)	Reference
Goethite	3.83	[33]
Perlite	0.64	[34]
Natural zeolites	5.17	[35]
Sepiolite	5.69	[16]
Montmorillonite	6.30	[36]
Pure smectite	3.87	[37]
Raw kaolinite	0.703	[38]
Phosphate	1.7–7.5	[39]
Kaolinite	6.80	[16]
Bentonite	8.45	[40]
Vermiculite	0.099	[41]
Goethite	1.07	[42]
Nigerian bentonite	4.08	[43]
Brasgel clay	0.84	[44]
QC-MT	5.85	This work
QC-MC	4.23	This work

clays (illite, smectite, montmorillonite, etc.), carbonates (calcite, dolomite, etc.), and phosphate (apatite) [32]. Clays have permanent charges (isomorphic substitutions) and load variables of silanol groups and aluminol groups also of iron oxide group and aluminum oxide group, which give them the ability to fix an inclusive variety of cadmium. However, this fixation of Cd (II) ions to the surface of the adsorbents under the effect of the negative electrical charges present on the surface formed an internal sphere complex between the adsorbent and cadmium ions. Recently, researchers have used clay minerals to remove cadmium ions from an aqueous solution like kaolinite, montmorillonite, bentonite, and other clays raw. Table 5 gathers some adsorbents and their adsorption capacity reported in the literature. These results show that these adsorbents have a remarkable adsorption capacity compared to other absorbents used for the treatment of Cd (II) ions, which makes them alternatives and good adsorbents for the Cd (II) ions.

4. Conclusion

In summary, both natural clays from the Middle Atlas region in Morocco were successfully analyzed and applied for the treatment of aqueous medium contaminated by Cd (II) ions heavy metal. The quantity of Cd (II) ions adsorbed on both natural clays is found to increase with the increase in the adsorbent dose, pH of the solution, initial heavy metal concentration, contact time, and temperature. The kinetic study revealed that the adsorption mechanism can be described by a pseudo-second-order model. The isotherm data indicated that the nature of Cd (II) ions adsorption onto both natural clays is described by the Freundlich model, thus indicating multilayer adsorption of Cd (II) ions on heterogeneous active sites of both natural clay adsorbents. The maximum Cd (II) ions adsorption capacity is 5.85 mg/g for QC-MT and 4.23 mg/g for QC-MC at 25°C. The thermodynamic study allowed concluding that the Cd (II) adsorption onto QC-MC and QC-MT was exothermic, favorable, and spontaneous. The regeneration tests suggested that hydrochloric acid was most effective in desorbing Cd (II) ions from the surface of QC-MC and QC-MT. The results of the adsorption process indicated that both Moroccan natural clays are effective and low-cost natural adsorbents for the purification of aqueous environments polluted by Cd (II) ions.

Data Availability

The datasets used and analyzed during the current study are available from the corresponding author upon request.

Conflicts of Interest

The authors declare that they have no known competing financial interests or personal relationships that could have appeared to influence the work reported in this article.

Acknowledgments

This work has been possible by following the assistance of several people. The authors thank everyone who helped and contributed to the development of this research.

References

[1] E. H. Elkhattabi, M. Lakraimi, M. Berraho, A. Legrouri, R. Hammal, and L. El Gaini, "A new nanostructured material based on fluorophosphate incorporated into a zinc-aluminium layered double hydroxide by ion exchange," *Bulletin of Materials Science*, vol. 40, no. 4, pp. 745–751, 2017.

[2] H. Karym, J. Maissara, M. E. M. Chbihi, M. Moutaabbid, and S. Benmokhtar, "Adsorption of dyes on mineral surfaces: a study of adsorption capacity of phyllosilicates," *European Journal of Biomedical and Pharmaceutical Sciences*, vol. 5, 2018.

[3] S. EL Makhloufy, M. Tridane, E. M. Majdi et al., "Chemical preparation, thermal behavior and infrared studies of the new cyclotriphosphate tetrahydrate of manganese and distrontium, MnSr2(P3O9)2.4H2O," *Mediterranean Journal of Chemistry*, vol. 9, no. 4, pp. 280–289, 2019.

[4] E. H. Elkhattabi, M. Lakraimi, M. Badreddine, A. Legrouri, O. Cherkaoui, and M. Berraho, "Removal of Remazol Blue 19 from wastewater by zinc-aluminium-chloride-layered double hydroxides," *Applied Water Science*, vol. 3, no. 2, pp. 431–438, 2013.

[5] E. H. Mourid, M. Lakraimi, L. Benaziz, E. H. Elkhattabi, and A. Legrouri, "Wastewater treatment test by removal of the sulfamethoxazole antibiotic by a calcined layered double hydroxide," *Applied Clay Science*, vol. 168, pp. 87–95, 2019.

[6] S. E. Bailey, T. J. Olin, R. M. Bricka, and D. D. Adrian, "A review of potentially low-cost sorbents for heavy metals," *Water Research*, vol. 33, no. 11, pp. 2469–2479, 1999.

[7] M. Belhabra, I. Fahim, A. Atibi et al., "Vibrational study and thermal behavior of dihydrogenotriphosphate trihydrate of 4-aminobenzoic acid and its anhydrous new form fertilizer type NP," *Mediterranean Journal of Chemistry*, vol. 8, no. 4, pp. 270–282, 2019.

[8] M. Belhabra, S. Zerraf, A. Kheireddine et al., "Structural and vibrational study of diphenylhydrazine dihydrogenophosphate single crystal (C 6 H 9 N 2) 2 H 2 P 2 O 7 (DPHDP)," *Chemical Data Collections*, vol. 13-14, pp. 73–83, 2018.

[9] E. H. Elkhattabi, M. Lakraimi, M. Berraho, A. Legrouri, R. Hammal, and L. El Gaini, "Acid Green 1 removal from wastewater by layered double hydroxides," *Applied Water Science*, vol. 8, no. 1, p. 45, 2018.

[10] N. K. Lazaridis, T. D. Karapantsios, and D. Georgantas, "Kinetic analysis for the removal of a reactive dye from aqueous solution onto hydrotalcite by adsorption," *Water Research*, vol. 37, no. 12, pp. 3023–3033, 2003.

[11] J. Maissara, H. Karym, M. E. M. Chbihi et al., "Chemical stabilization with lime of expansive clays from northern Morocco," *International Journal of Trend in Research and Development*, vol. 3, p. 6, 2016.

[12] A. Atibi, K. El Kababi, M. Belhabra, S. Zerraf, M. Tridane, and S. Belaaouad, "Chemical preparation, crystal structure and vibrational study of a new dihydrogenotriphosphate trihydrate of 4-aminobenzoic acid fertilizer type NP," *Journal of Coordination Chemistry*, vol. 71, no. 21, pp. 3510–3520, 2018.

[13] E. H. Elkhattabi, M. Badreddine, M. Berraho, and A. Legrouri, "Incorporation of fluorophosphate into zinc-aluminium-nitrate layered double hydroxide by ion exchange," *Bulletin of Materials Science*, vol. 35, no. 4, pp. 693–700, 2012.

[14] I. Ghorbel-Abid and M. Trabelsi-Ayadi, "Competitive adsorption of heavy metals on local landfill clay," *Arabian Journal of Chemistry*, vol. 8, no. 1, pp. 25–31, 2015.

[15] R. A. K. Rao and M. Kashifuddin, "Adsorption studies of Cd(II) on ball clay: comparison with other natural clays," *Arabian Journal of Chemistry*, vol. 9, pp. S1233–S1241, 2016.

[16] S. Sen Gupta and K. G. Bhattacharyya, "Immobilization of Pb(II), Cd(II) and Ni(II) ions on kaolinite and montmorillonite surfaces from aqueous medium," *Journal of Environmental Management*, vol. 87, no. 1, pp. 46–58, 2008.

[17] V. B. Yadav, R. Gadi, and S. Kalra, "Clay based nanocomposites for removal of heavy metals from water: a review," *Journal of Environmental Management*, vol. 232, pp. 803–817, 2019.

[18] H. Saufi, M. E. Alouani, J. Aride, and M. h. Taibi, "Rhodamine B biosorption from aqueous solution using *Eichhornia crassipes* powders: isotherm, kinetic and thermodynamic studies," *Chemical Data Collections*, vol. 25, Article ID 100330, 2020.

[19] M. El Alouani, H. Saufi, G. Moutaoukil et al., "Application of geopolymers for treatment of water contaminated with organic and inorganic pollutants: state-of-the-art review," *Journal of Environmental Chemical Engineering*, vol. 9, no. 2, Article ID 105095, 2021.

[20] E. N. Bakatula, D. Richard, C. M. Neculita, and G. J. Zagury, "Determination of point of zero charge of natural organic materials," *Environmental Science and Pollution Research*, vol. 25, no. 8, pp. 7823–7833, 2018.

[21] S. Dudek and D. Kołodyńska, "Enhanced arsenic(V) removal on an iron-based sorbent modified by lanthanum(III)," *Materials*, vol. 13, no. 11, p. 2553, 2020.

[22] P. N. Fotsing, E. D. Woumfo, S. Mezghich et al., "Surface modification of biomaterials based on cocoa shell with improved nitrate and Cr(vi) removal," *RSC Advances*, vol. 10, no. 34, pp. 20009–20019, 2020.

[23] S. Belaaouad, A. Charaf, K. E. Kababi, and M. Radid, "Chemical preparation, crystallographic characterization, thermal behavior and IR studies of two new cyclotriphosphates SrKP3O9·3H2O and SrKP3O9," *Journal of Alloys and Compounds*, vol. 468, no. 1–2, pp. 270–274, 2009.

[24] T. H. Ko and H. Chu, T. H. Ko and H. Chu, Spectroscopic study on sorption of hydrogen sulfide by means of red soil," *Spectrochimica Acta Part A: Molecular and Biomolecular Spectroscopy*, vol. 61, no. 9, pp. 2253–2259, 2005.

[25] K. Sbai, S. Belaaouad, A. Abouimrane, and M. Moutaabbid, "Chemical preparation, crystallographic characterization, thermal behavior and IR studies of a new cyclotriphosphate SrTlP3O9·3H2O," *Materials Research Bulletin*, vol. 37, no. 5, pp. 915–924, 2002.

[26] S. Belaaouad, K. Sbai, A. Kenz, and M. Pierrot, "Chemical preparation, thermal behavior and crystal structure of ammonium barium cyclotriphosphate dihydrate," *Materials Research Innovations*, vol. 3, no. 6, pp. 352–359, 2000.

[27] K. Sbai and S. Belaaouad, "Chemical preparation, crystal structure, thermal behavior and IR studies of barium thallium cyclotriphosphate dihydrate," *Journal of Physics and Chemistry of Solids*, vol. 64, no. 6, pp. 981–991, 2003.

[28] M. Singha and L. Singh, "Vibrational spectroscopic study of muscovite and biotite layered phyllosilicates," *Indian Journal of Pure and Applied Physics*, vol. 54, 2016.

[29] M. Tridane, S. Belaaouad, and K. Sbai, "Chemical preparations and crystal data for eight new condensed phosphates," *Solid State Sciences*, vol. 2, no. 7, pp. 701–704, 2000.

[30] I. Fahim, M. Tridane, and S. Belaaouad, "An experimental and theoretical correlation of inhibition effect of some dihydropyridine on mild steel in 1 M HCL an experimental and theoretical correlation of inhibition effect of some dihydropyridine on mild steel in 1 M HCL," *The European Physical Journal-Applied Physics*, vol. 93, 2021.

[31] N. A. Ndukwe and F. O. Jenmi, "Effects of vehicular exhaust fumes on urban air pollution in Lagos Metropolis," *Pollution Research*, vol. 27, 2018.

[32] S. Belaaouad and K. Sbai, "Chemical preparation and crystal data for two new condensed phosphates," *Powder Diffraction*, vol. 17, no. 1, pp. 23-24, 2002.

[33] T. Tang, C. Yang, L. Wang, X. Jiang, Z. Dang, and W. Huang, "Complexation of sulfamethazine with Cd(II) and Pb(II): implication for co-adsorption of SMT and Cd(II) on goethite," *Environmental Science and Pollution Research*, vol. 25, no. 12, pp. 11576–11583, 2018.

[34] T. Mathialagan and T. Viraraghavan, "Adsorption of cadmium from aqueous solutions by perlite," *Journal of Hazardous Materials*, vol. 94, no. 3, pp. 291–303, 2002.

[35] S. M. D. Bosco, R. S. Jimenez, C. Vignado et al., "Removal of Mn(II) and Cd(II) from wastewaters by natural and modified clays," *Adsorption*, vol. 12, no. 2, pp. 133–146, 2006.

[36] S. M. D. Bosco, "Pontifícia universidade católica do rio grande do sul programa de pós-graduação em gerontologia biomédica," vol. 127, 2006.

[37] K. Bedoui, I. Bekri-Abbes, and E. Srasra, "Removal of cadmium (II) from aqueous solution using pure smectite and Lewatite S 100: the effect of time and metal concentration," *Desalination*, vol. 223, no. 1–3, pp. 269–273, 2008.

[38] E. Godwin Ogbaji, B. Nwunuji Hikon, N. Godfrey Sheckhar et al., "Synergistic study of hydroxyiron (III) and kaolinite composite for the adsorptive removal of phenol and cadmium," *International Journal of Environmental Chemistry*, vol. 3, no. 1, p. 30, 2019.

[39] M. I. Kandah, "Zinc and cadmium adsorption on low-grade phosphate," *Separation and Purification Technology*, vol. 35, no. 1, pp. 61–70, 2004.

[40] Z. Q. Hu, X. H. Yang, and Y. C. Zhang, "Clay minerals as a feasible additive to stabilize cadmium in contaminated soils," *Key Engineering Materials*, vol. 336–338, 2007.

[41] K. Vijayaraghavan and F. D. Raja, "Pilot-scale evaluation of green roofs with Sargassum biomass as an additive to improve runoff quality," *Ecological Engineering*, vol. 75, pp. 70–78, 2015.

[42] B. Dash, B. Dash, and S. S. Rath, "A thorough understanding of the adsorption of Ni (II), Cd (II) and Zn (II) on goethite using experiments and molecular dynamics simulation," *Separation and Purification Technology*, vol. 240, p. 116649, 2020.

[43] J. A. Alexander, M. A. A. Zaini, S. Abdulsalam, U. Aliyu El-Nafaty, and U. O. Aroke, "Isotherm studies of lead(II), manganese(II), and cadmium(II) adsorption by Nigerian bentonite clay in single and multimetal solutions," *Particulate Science & Technology*, vol. 37, no. 4, pp. 403–413, 2019.

[44] J. D. Mota and R. S. Souza Cunha, "Cadmium adsorption kinetic study using natural brasgel clay the adsorbent," *Materials Science Forum*, vol. 912, pp. 202–206, 2018.